The 2013 World Congress on
Advances in Nano, Biomechanics, Robotics, and Energy Research (ANBRE13)
Seoul, Korea, August 25-28, 2013

A Comparative Study of Anti-islanding Control Techniques for Grid-connected Photovoltaic Systems

*Wei Yee TEOH[1)] and Chee Wei TAN[2)]
[1),2)] *Department of Electrical Power, Faculty of Electrical Engineering, Universiti Teknologi Malaysia (UTM), 81310 Skudai Johor, Malaysia.*
[1)]*weiyee@fkegraduate.utm.my*
[2)]*cheewei@fke.utm.my*

ABSTRACT

Photovoltaic (PV) is one of the popular choice among the DGs, which typically establishes in grid-connected systems. However, for grid-connected systems, the issue of unintentional islanding remains as a great challenge. In order to enhance the PV grid-connected technologies, the phenomenon of unintentional islanding is typically avoided by anti-islanding detection controller. This paper presents the comparative study of anti-islanding detection techniques which include passive, active and the proposed hybrid technique. The principle of operation for both the passive and active anti-islanding detection techniques, namely Voltage and frequency Protection (OVP/UVP and OFP/UFP) and Active Frequency Drift (AFD) are described. In addition to that, the integration of these techniques which form the proposed hybrid anti-islanding detection technique will be explained. In this work, the performances of the studied anti-islanding techniques are simulated using MATLAB/Simulink package. The proposed hybrid technique applies two-phase detection, where the passive detection is used as the main protection and followed by the active detection. Finally, the results of simulation show that the proposed hybrid anti-islanding detection technique is able to achieve higher detection efficiency as compared to single detection techniques. The improvements include a narrower non-detected zone, faster response time and better power quality.

Keyword - Photovoltaic (PV) grid-connected system; islanding detection; passive method; active method; hybrid method, Voltage and frequency protection (OVP/UVP and OFP/UFP), Active frequency drift (AFD)

1. INTRODUCTION

In the age of technological advancement, rapid development of industrialization, energy consumption is correspondingly skyrocketed. This scenario has led to gradual exhaustion of resources as well as poses serious environmental pollution. (M.Asif (2007)). Therefore, deployments of green energy systems have gained tremendous attention worldwide in recent years. This in turns has brought rapid development in distributed generation. However, the issue of islanding still remains as a challenge in distributed generations. Therefore, the research of islanding detection technology is essential and important. According to the definition as given by the IEEE Standard 929-2000 (IEEE (2000)), islanding is a condition in which a portion of the utility system that contains both load and distributed resources remains energized while isolated from the remainder of the utility system. The islanding phenomena must be detected immediately and also grid should be stopped from energizing in order to protect the section from any damage. This action is performed at the Point of Common Coupling (PCC) which is known as Anti-islanding (IEEE (2000) ; IEEE (2009)).

This paper presents the comparative study of anti-islanding detection techniques to enhance the PV grid-connected systems. Anti-islanding detection techniques discussed in this paper include the passive, active and the proposed hybrid techniques. The former technique is the under voltage and over voltage protection (UVP/OVP) and under frequency and over frequency protection (UFP/OFP) while the latter detection technique is active frequency drift (AFD). In addition to that, the integration of these techniques which form the proposed hybrid anti-islanding detection technique will be explained. In this work, the performances of the studied anti-islanding techniques are simulated using MATLAB/Simulink package. Finally, the simulation results will be analyzed and discussed.

2. ISLANDING DETECTION TECHNIQUES

According to grid interconnection standard (AS (2005) ; IEEE (2000) ; IEEE (2003) ; IEEE (2009)), the voltage and the frequency protection is to provide a basic protection to grid-connected DGs. For this reason, the passive technique selected for this proposed hybrid technique are the voltage and frequency protection which are UFP/OFP and UVP/OVP techniques. However, the active method selected is Active Phase Drift (AFD) because of the technique is easy to implement in a small scale system, with less cost and

extremely fast anti-islanding detection time. The passive, active and the proposed hybrid islanding detection techniques are explained in detail in the following sections.

2.1 Passive islanding detection technique: Frequency and Voltage Protection

The UFP/OFP and UVP/OVP are also known as the standard protective relay or abnormal voltage detection. This method is used as a fundamental protection for the PV grid-connected system which is essential to all grid-connected PV systems. This is to ensure that the DG stops injecting power into the utility in cases where the PCC voltage amplitude (V_{PCC}) or the frequency (F_{PCC}) exceeds the defined thresholds. Hence, besides protection, the OFP/UFP and OVP/UVP method also serves as anti-islanding detection method (IEEE (2000)).

The power flow of grid connected PV system and the point of common coupling (PCC) are shown in Fig. 1. The PCC is located between the utility grid and Power Conditioning Unit (PCU) of a PV DGs. Under normal operation mode, there closer is closed in which the utility is connected to the PV system.

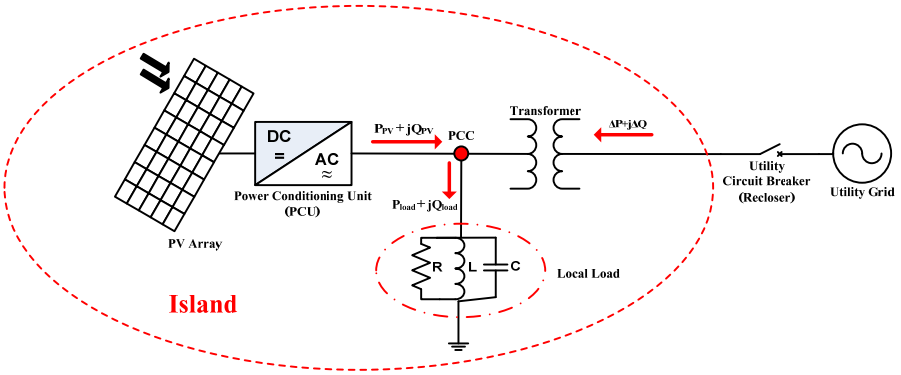

Fig. 1 The power flow in a PV grid-connected system under a normal operating condition.

The active power demand for the local load (P_{load}) and active power generating from PV system (P_{PV}) are not matched at the time when the grid is disconnected. At this point, The V_{PCC} must increase or decrease until $P_{PV} = P_{load}$. Similarly, if the reactive power demands of local load (Q_{load}) and reactive power generating (Q_{PV}) are not matched at the time when the grid is disconnected. The F_{PCC} must be changed until the $Q_{PV} = Q_{load}$. The PV inverter will seek for a frequency at which the current-voltage phase angle of the local load equals to the phase angle of the PV system. Therefore, the voltage and frequency changes can be detected by the UFP/OFP and UVP/OVP relays (Skocil (2009)).

However, when a local load demand and the PV generation are closed, it is difficult to detect an islanding because of the small values of power variation (ΔP). At the same time, there active power variation (ΔQ) for NDZ is insufficient for the frequency or voltage

changes to be detectable by the UFP/OFP and UVP/OVP relays. In this case, the OVP/UVP protection will not be triggered to trip the utility and hence islanding is not prevented. The power mismatch, voltage and frequency relationship can be expressed in Eq. (1) and Eq. (2).

$$\left[\frac{V_{ref}}{V_{max}}\right]^2 - 1 \leq \frac{\Delta P}{P} \leq \left[\frac{V_{ref}}{V_{min}}\right]^2 - 1 \quad (1)$$

$$Q_f\left[1 - \left(\frac{f_{ref}}{f_{min}}\right)^2\right] \leq \frac{\Delta Q}{P} \leq Q_f\left[1 - \left(\frac{f_{ref}}{f_{max}}\right)^2\right] \quad (2)$$

Fig. 2 shows the NDZ determined from Eq. (1) and Eq. (2) for 88%-110% of PCC V_{RMS} and 98.83%-100.83% of PCC frequency. The differentiation between a grid connected condition and islanding is based on the parameters thresholds setting of voltage and frequency limits. Extreme care should be taken while setting the values of the thresholds, so as to effectively differentiate islanding from other disturbances in the system

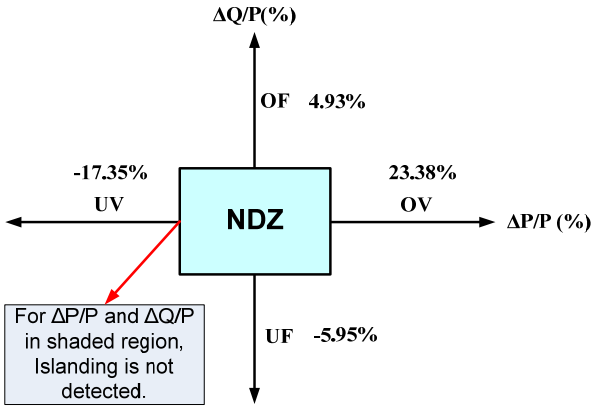

Fig. 2 The NDZ for 88%-110% of V_{PCC_rms} and 98.83%-100.83% of F_{PCC}.

It is necessary to develop islanding techniques which are suitable for cases when the powers of PV and local load are closely matched. It is the aim of all islanding detection methods to reduce the NDZ as close to zero as possible (Ward Bower (2002a)). The detailed theoretical explanations for VFP can be found in *(A. S. Aljankawey (2010) ; Mylène Robitaille (2011) ; Skocil (2009) ; Velasco (2010) ; Ward Bower (2002a)).*

2.2 Active islanding detection technique: Active Frequency Drift

The AFD is a technique that forces a slightly higher frequency bias signal into the grid current via PCC compare to grid voltage (Luiz A.C.Lopes (2006)). This technique is also known as Frequency bias, where the method employs positive feedback by creating be

slightly misaligned the phase angle of inverter output current. However, the power factor remains closer to the utility grid, and resets itself every half cycle, as shows in Fig. 3.

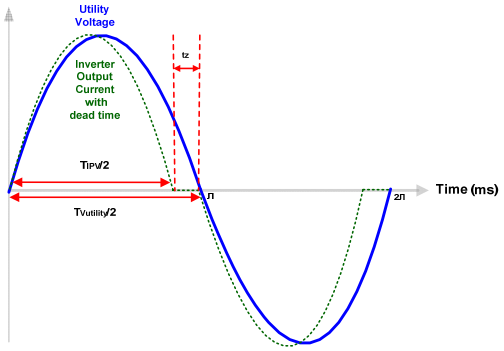

Fig.3 The distorted current waveform for the AFD islanding detection technique.

The inverter phase angle (ϕ_{PV}) is given by Eq. (3) (Luiz A.C.Lopes (2006)).

$$\emptyset_{PV} = \pi f t_Z = \frac{\pi \delta_f}{f_n + \delta_f} \tag{3}$$

where t_Z is a dead time or zero time, δ_f is forcing current frequency and f_n is nominal frequency. Based on Fig. 3, the T_{IPV} is the period of one cycle sinusoidal inverter current output waveform while the $T_{Vutility}$ is the period of one cycle sinusoidal utility voltage waveform. The chopping fraction (Cf) is defined inEq. (4) (Ward Bower (2002b)).

$$cf = \frac{2t_z}{T_{Vutility}} \tag{4}$$

During the first half-cycle, the PV inverter current output is a sinusoid with a frequency slightly higher than the utility voltage. When the PV inverter output current reaches zero crossing, it remains at zero for time t_Z before beginning the second half cycle. At the first part of the second half-cycle, the PV inverter output current is the negative half of the sine wave from the first half-cycle. When the PV inverter current again reaches zero, it remains at zero until the rising zero crossing of the utility voltage. It is important to note that the zero time in the second half cycle is not fixed and does not equals t_Z (Ward Bower (2002b)).

If the utility grid is connected, the Cf is low because the utility grid stabilizes the V_{PCC} by providing a solid phase and frequency reference. Once the utility grid is disconnected, there is a phase error between V_{PCC} and $i_{PV\text{-}inv}$ waveforms (Kunte (2008)). The PV inverter will increase the frequency of $i_{PV\text{-}inv}$ in order to eliminate the phase error. The zero crossing of voltage response of the load again advances in time with respect to where it was expected to be, and the PV inverter still detects a phase error and increases its frequency (Ward Bower (2002a)). This repetitive cycle results in a constant increase in the value of

the Cf, until the frequency has drifted far enough from ω_0 to be detected by the OFP/UFP. Once detected, it will be triggered to stop the inverter from operation. .

2.3 Proposed hybrid islanding detection technique

Based on current research on hybrid anti-islanding detection techniques, most of the hybrid methods proposed in literatures are applied in synchronous machines and three phase systems. The proposed algorithm is a hybrid islanding protection technique which combines passive and active anti-islanding control algorithms to effectively control anti-islanding for a small scale grid-connected PV system that less than 1 kW. The objective of the proposed technique is to reduce the NDZ and also improve the power quality in the way reduce the harmonic contented in the output power. The idea of the technique is first PV grid-connected system primary protecting by VFP. In this primary stage, the VFP techniques hold the advantage of passive islanding detection techniques. Thus, for those cases that out of the NDZ range islanding can be detected with good power quality.

However, in the cases where the passive method during the primary stage failed to detect islanding within the NDZ, the second stage detection will be triggered. At this point, the AFD begins to operate as explained in section 2.2.

3. RESULTS AND DISCUSSION

Simulation model of the VFP, AFD and the proposed islanding detection techniques have been done in Simulink.

3.1 Simulation Module and result: VFP

The simulation was made by referring to the IEEE standard in (IEEE (2000)), where the normal operating voltage at the PCC is in between 88%-110% of the grid voltage; the frequency at the PCC is in the range of 98.83%-100.83% of grid frequency. The islanding detection limits for a grid supply 240 V / 50 Hz are listed in Table 1. Hence, the operation window is 211 V - 264 V on a 240 V base, so voltage protection tripping point will be set at 210 V and 265 V, respectively. The frequency test points for determining proper operation of the frequency trip function should be 49.3 Hz and 50.5 Hz respectively. The VFP mapping is shown in Fig. 4. The simulation model has been developed to test the frequency and the root min square voltage (V_{RMS}) at the PCC, which the grid disconnection was set at t=0.5 s. Therefore, the clearing time for UFP/OFP detection must less than t=0.62 s, and the UVP/OVP detection time must less than t=2.9 s.

Table 1. The grid voltage and frequency limits for VFP.

Standard	Voltage at PCC		Clearing Time	Frequency at PCC	Clearing Time	Quality Factor	Power Quality	
	V_{RMS}			Hz				
system >30kW	(% of base voltage)	(Base voltage 240V)	Cycle	Utility frequency 50Hz	Cycle	Qf	THDv	THDi
IEEE 929-2000	V<50	V<110	6	f<49.4 f>50.4	6	2.5	<5%	<5%
	50≤V<88	110≤V<211	120					
	88≤V≤110	211≤V≤264	Normal					
	110<V<137	264<V<329	120					
	137≤V	329≤V	2					

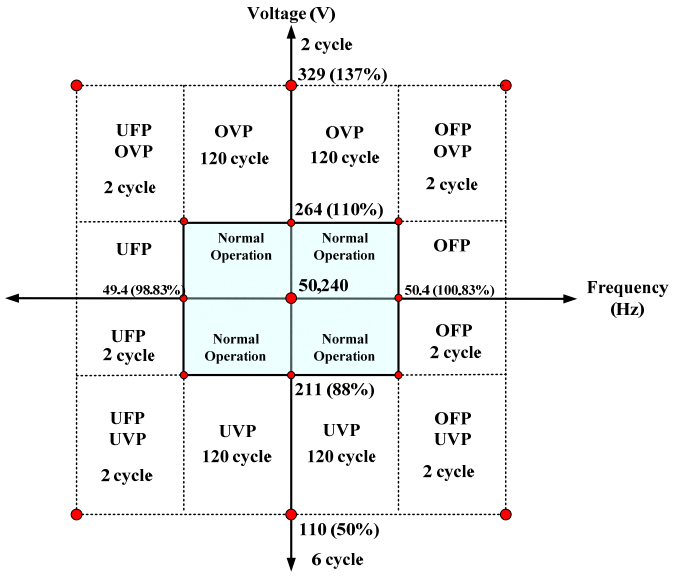

Fig. 4 The VFP mapping for a 240 V / 50 Hz system.

Fig. 5 shows the operating flow-chart and Fig.6 shows the simulation model for the OVP/UVP and OFP/UFP anti-islanding control. The control system designed to monitoring the voltage and frequency at the PCC, and stop supply to the local load if voltage and frequency out of indicated threshold state in Table 1.

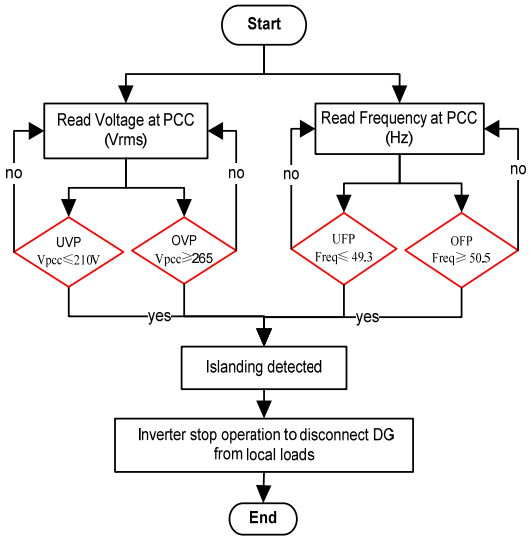

Fig. 5 The VFP operating flow-charts.

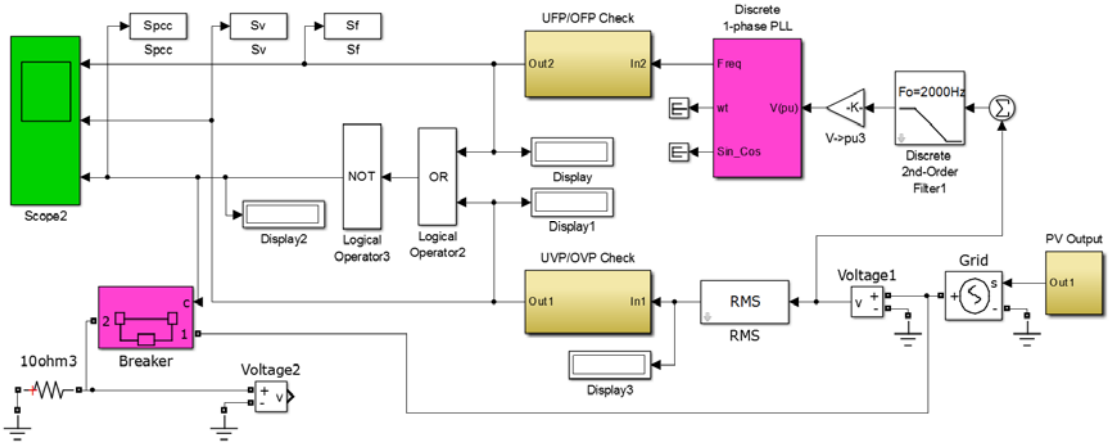

Fig. 6 The VPF simulation model.

Fig. 4 shows the various cases of voltage and frequency condition that have been simulated using the simulation module. The V_{PCC} and F_{PCC} were set at the accepted and reference value respectively, in order to detect any abnormal voltage and frequency at the PCC when islanding happens. The simulation result fulfills the the 6 cycles (0.12s) clearing time in detecting abnormal voltage or frequency. In addition, the simulation results show that longer time are required to trigger an islanding detection for abnormal frequencies with values close to the threshold value. However, a large NDZ falling within the threshold limit causes the VFP fails to detect islanding. The simulated output waveforms for normal

operation are shown in Fig.7 and Fig. 8. The output waveforms for the case of under frequency are shown in Fig.9 and Fig. 10, while the results for the case of over frequency are presented in Fig.11 and Fig. 12.

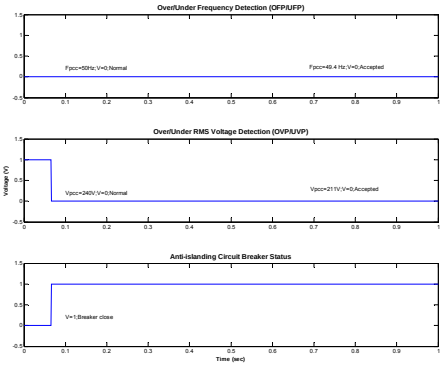

Fig.7 The detection signals for VFP under the normal operation: V_{PCC}=211 V F_{PCC}=49.4 Hz
(a) OFP/UFP checker: V=0
(b) OVP/UVP checker: V=0
(c) Circuit breaker does not detect any abnormality.

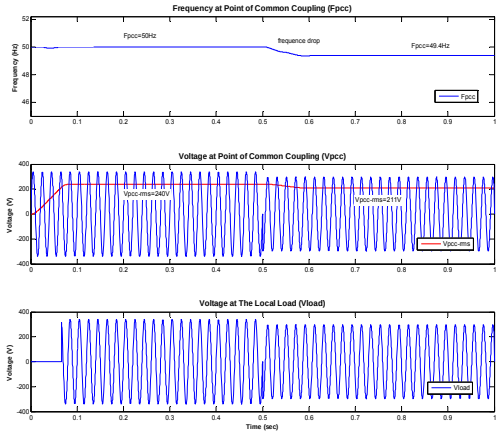

Fig.8 The simulation result for VFP at the normal operation
(a) Frequency at PCC; Fpcc=49.4 Hz
(b) Peak–peak voltage ($V_{PCC\_p\text{-}p}$) and RMS voltage at PCC : V_{PCC_rms}=211 V
(c) Load Voltage (V_{load}): inverter continues supplying the load.

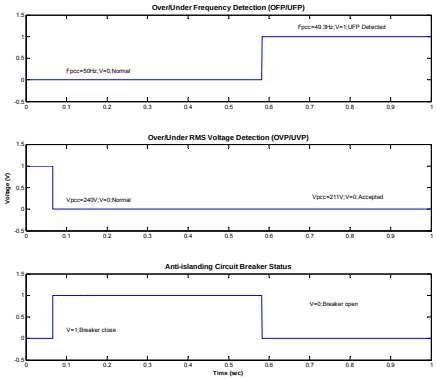

Fig.9 The detection signals for VFP under the UFP operation: V_{PCC}=211 V F_{PCC}=49.3 Hz
(a) OFP/UFP checker trigger UFP at t=0.5824 s: V=1
(b) OVP/UVP checker: V=0
(c) Circuit breaker opens at t=0.5824 s.

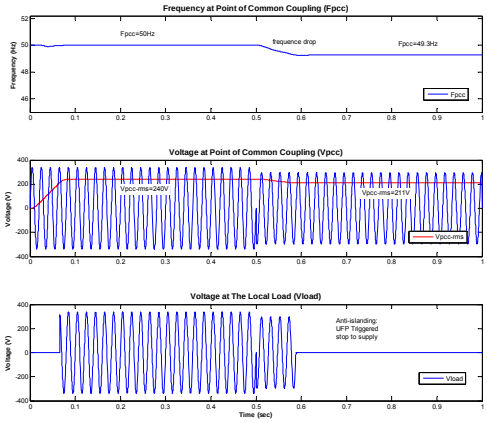

Fig.10 The simulation result for VFP under the UFP operation
(a) Frequency at PCC; F_{PCC}=49.3 Hz
(b) Peak–peak voltage ($V_{PCC\_p\text{-}p}$) and RMS voltage at PCC : V_{PCC_rms}=211 V
(c) Load Voltage (V_{load}):Inverter stops supplying to the load at t=0.5882 s

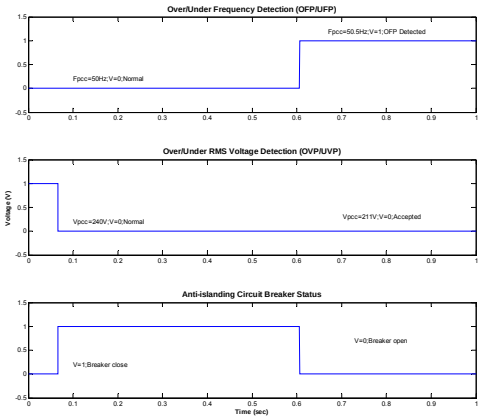

Fig.11 The detection signals for VFP under the OFP operation: V_{PCC}=211 V F_{PCC}=50.5 Hz
(a) OFP/UFP checker trigger OFP at t=0.6062 s: V=1
(b) OVP/UVP checker: V=0
(c) Circuit breaker opens at t=0.6062 s.

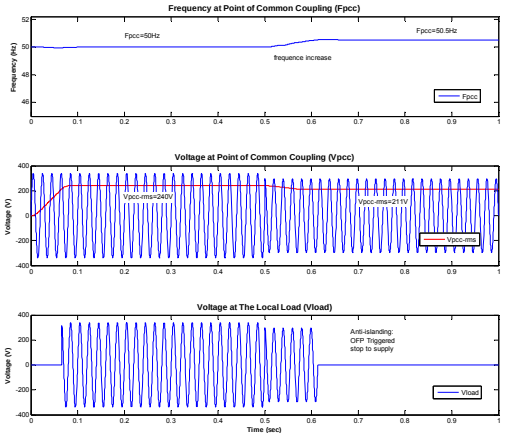

Fig.12 The simulation result for VFP under the OFP operation
(a) Frequency at PCC; F_{PCC}=50.5 Hz
(b) Peak–peak voltage ($V_{PCC\_p\text{-}p}$) and RMS voltage at PCC : V_{PCC_rms}=211 V
(c) Load Voltage (V_{load}):Inverter stops supplying to the load at t=0.6140 s

3.2. Simulation block and result: Active Frequency Drift

According to the AFD theoretical explanation in section 2.2, a 1 kW single-phase PV power generation system is established in Matlab/Simulink. Fig.13 shows the simulation model for the AFD anti-islanding control. This control was designed to monitor the V_{PCC} and F_{PCC}. The control will produce a signal to the inverter to stop supplying to the local load if voltage and frequency are out of the limits as indicated in Table 1. The simulation

module includes the inverter circuit connected to a utility grid control and AFD islanding detection section at the PCC. The function of AFD controller module was achieved by using the s-function in Matlab/Simulink. The V_{PCC} and I_{pv_inv} are in phase at the initial setting. The DC voltage was set to be 400 V to represent the PV output; the grid supply was set to be 155 Vp-p / 50 Hz. The RL filter are L=6 mH and R=0.01 Ω, respectively. The threshold of frequency protection was set at 49.3 Hz and 50.5 Hz respectively. The Qf was set at 2.5, where the RLC load value were R=6.06 Ω, L=7.65 mH and C=1300 uF. The grid supply was set to be disconnected at t=0.1 s.

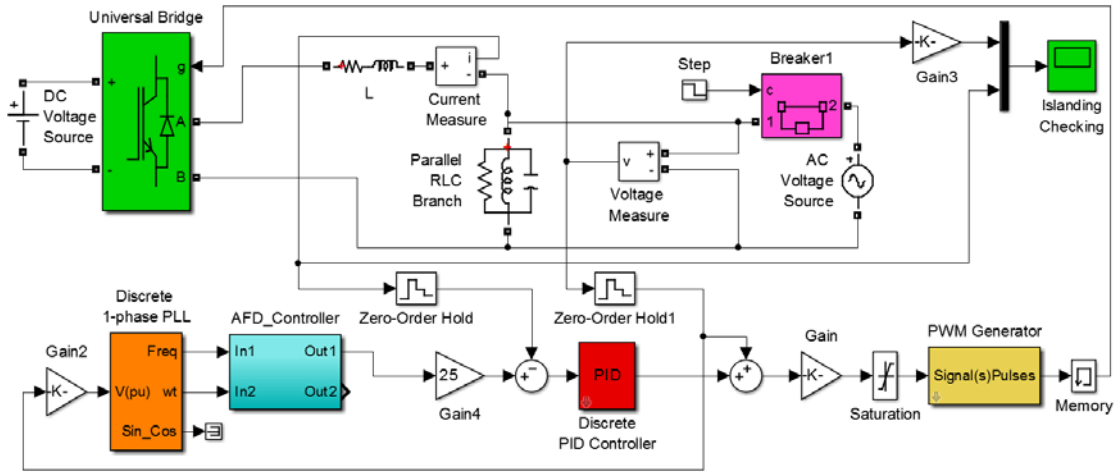

Fig.13 The simulation model of the AFD in Simulink.

Fig. 14 shows the flow diagram of the AFD detection algorithm. First, the frequency data was taken and tested against the UFP/OFP threshold, if it is not in the threshold, the islanding occurred, else it is not islanding. If there is no islanding, a source with frequency modified by the Cf is then injected into the inverter output current every half cycle and every full cycle to produce a t_Z on the output current waveform. The value of the Cf will slightly increase every half cycle to drift the current frequency from voltage frequency until islanding is detected and a signal will be sent to stop the inverter from operating.

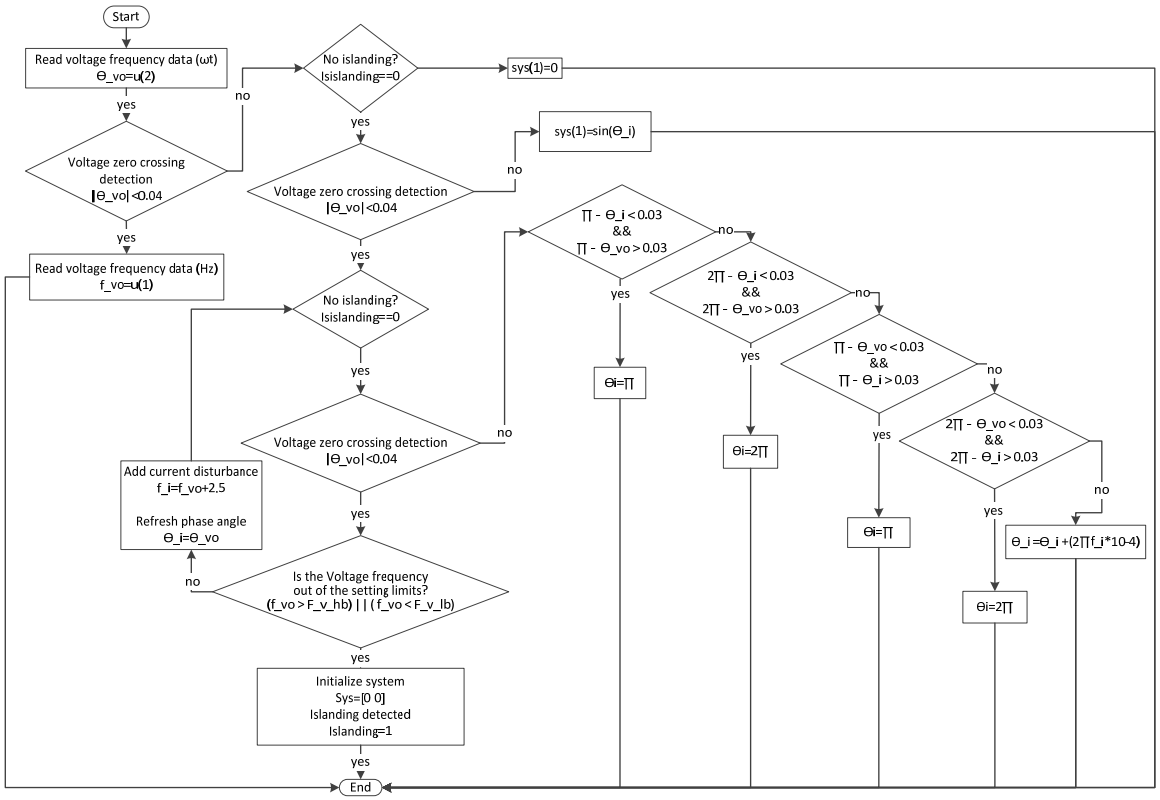

Fig. 14 The simulation flow-chart for the sub-block AFD_Controller.

A few test cases have been conducted using the simulation model built as shown in Fig. 13. Fig. 15-17 are the cases result for AFD controller which these cases were failed to be detected by the VFP within the NDZ. Fig.15 is the simulation output of AFD for the case F_{PCC}=49.4 Hz, Cf=0.049, the detection time t=0.1006 s and V_{PCC} fully stop at t=0.1594 s with the THD_i of 2.23%. Fig.16 is the case for F_{PCC}=50.0 Hz, Cf=0.05, the detection time t=0.1591 s and load V_{PCC} fully stop at t=0.2171 s with the THD_i of 3.91%. Fig.17 is the case for F_{PCC}=50.4, Cf=0.0504, the detection time t=0.1005 s and V_{PCC} fully stop at t=0.0.1672 s with the THD_i of 2.76%.

The results show that the AFD is capable of detecting islanding effectively with very small NDZ and a detection time within 0.06 s. The disturbance injection plays a significant role in performing islanding detection to meet the PV grid interconnection standard. The simulation results show the more disturbances injected the faster the islanding detection time but the higher the harmonic distortion.

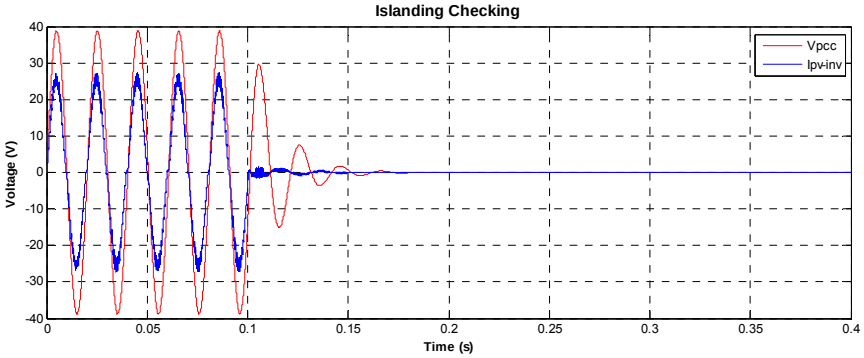

Fig.15 The simulation output of AFD for Frequency=49.4 Hz, Cf=0.049
Detection time, t=0.1006 s, V_{PCC} stop at t=0.1594 s

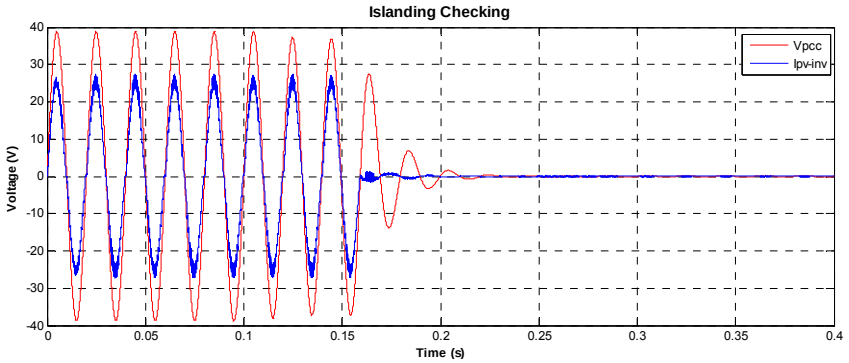

Fig.16 The simulation output of AFD for Frequency=50.0 Hz, Cf=0.05
Detection time, t=0.1591 s and load V_{PCC} stop at t=0.2171 s

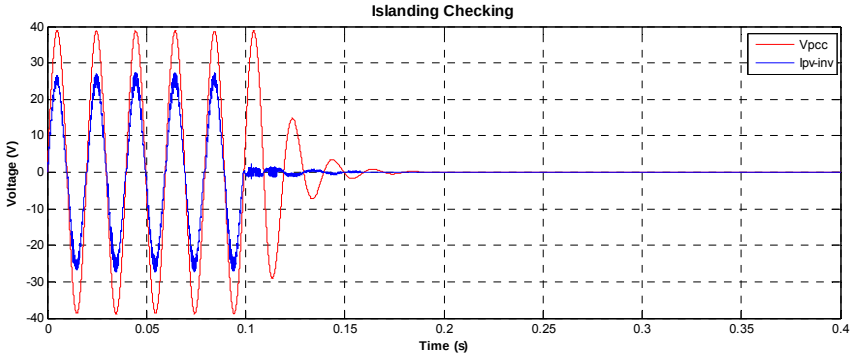

Fig.17 The simulation output of AFD for Frequency=50.4 Hz, Cf=0.0504
Detection time, t=0.1005 s and load V_{PCC} stop at t=0.0.1672 s

3.3 Simulation block and result: Proposed hybrid technique

The operating flow-chart of the proposed hybrid islanding detection technique is shown in Fig.18. The proposed technique for a PV grid-connected system is evaluated by the OVP/UVP and OFP/UFP in the first stage. If islanding is not detected in the primary stage, second stage will continue to evaluate the detection. In the second stage, the AFD controller produces a small disturbance signal to be injected into the output current of the inverter. If the grid is still connected to PCC, the small disturbance signal will be absorbed by the grid hence no islanding occurs. Otherwise, if the PCC is disconnected from the grid, the inverter current phase will drift from the V_{PCC} phase, hence islanding is detected. The simulation model of this proposed hybrid technique is shown in Fig.19, The parameters are the same as discussed the previous section.

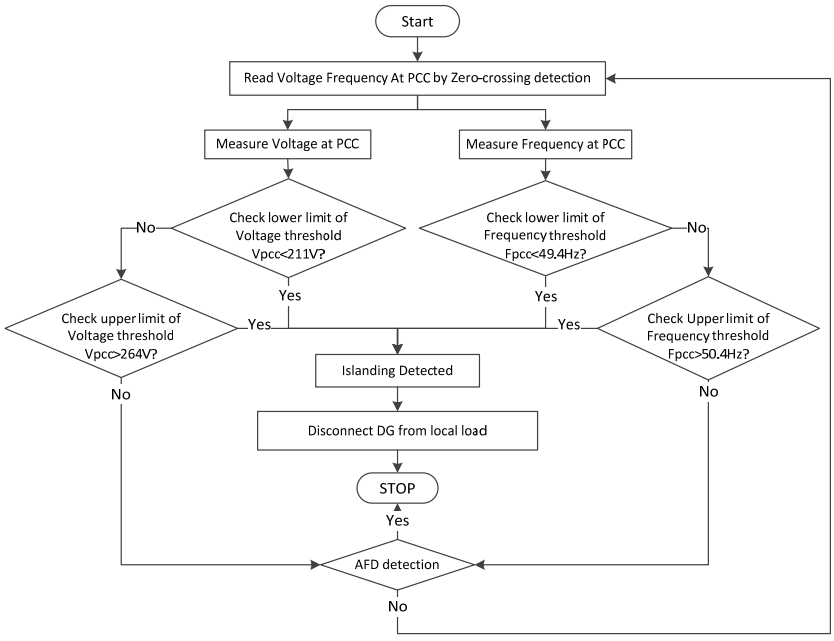

Fig. 18 The operating flow-chart for the proposed hybrid technique.

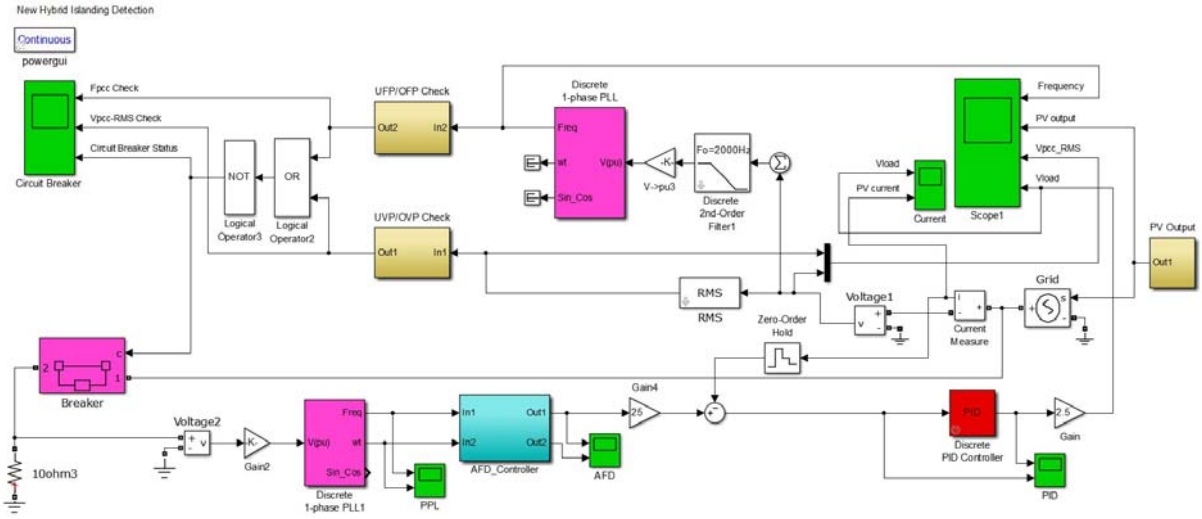

Fig.19 The simulation model for the proposed hybrid technique.

The proposed hybrid technique can effectively detected the islanding within the islanding detection clearing time and reduce the THD_i of the output waveform. Fig.20 and Fig. 21 show the simulation results for the case of F_{PCC} = 49.4 Hz, where islanding was detected at t=0.5658 s with THD_i of 1.17%. Fig.22 and Fig.23 show the simulation results for case F_{PCC} = 50.4 Hz Islanding detected at t=0.5950 s with THD_i of 2.00%.

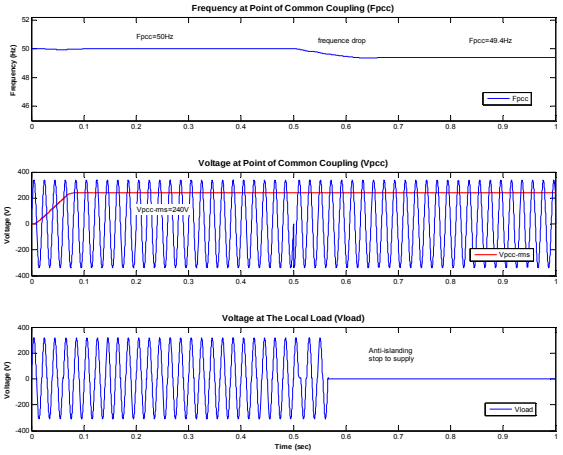

Fig.20 The hybrid technique simulation results: V_{PCC_rms}=240 V, F_{PCC}=49.4 Hz
(a) Frequency at PCC; F_{PCC}=49.4 Hz
(b) Peak–peak voltage ($V_{PCC\_p\text{-}p}$) and RMS voltage at PCC : V_{PCC_rms} =240 V
(c) Load Voltage (V_{load}): Inverter stops supplying to the load at t=0.5658 s

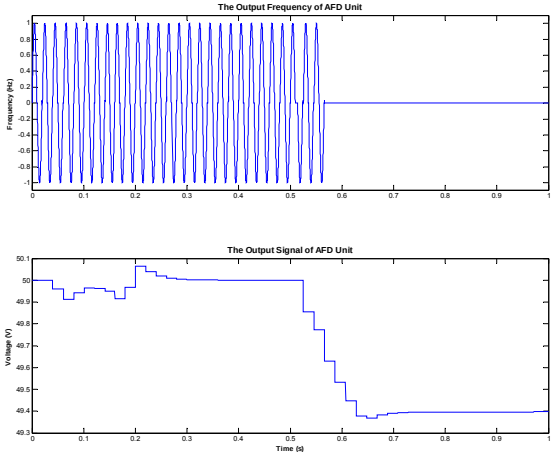

Fig.21 The AFD islanding controller signal: V_{PCC_rms}=240 V, F_{PCC}=49.4 Hz
(a) AFD detects islanding at t=0.5654 s
(b) The AFD frequency signal

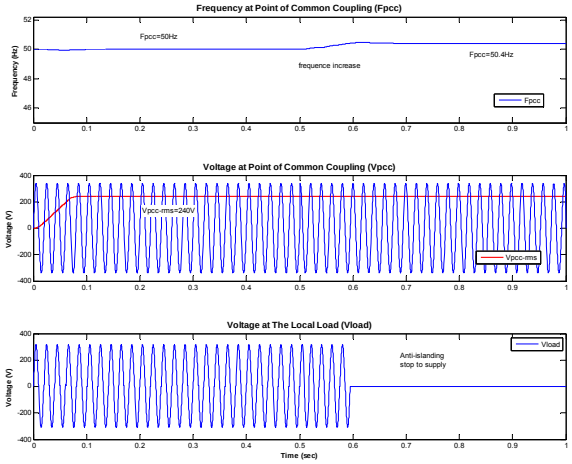

Fig.22 The hybrid technique simulation results: V_{PCC_rms}=240 V, F_{PCC}=50.5 Hz
(a) Frequency at PCC; F_{PCC}=50.5 Hz
(b) Peak–peak voltage ($V_{PCC\_p\text{-}p}$) and RMS voltage at PCC : V_{PCC_rms}=240 V
(c) Load Voltage (V_{load}): Inverter stops supplying to the load at t=0.5950 s

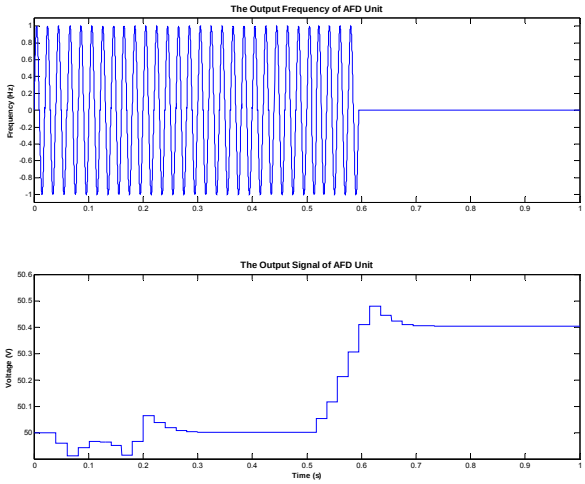

Fig.23 The AFD islanding controller signal: V_{PCC_rms} =211 V, F_{PCC}=50.4 Hz
(a) AFD detect islanding at t=0.5948 s
(b) The AFD frequency signal

4. CONCLUSIONS

This paper proposes a new hybrid anti-islanding detection technique, which combines passive anti-islanding detection technique (VFP) and active anti-islanding detection techniques (AFD). This technique is applies a two-phase detection, in which the passive detection is used as the main protection and followed by the active detection. The technique has been successfully simulated using MATLAB/Simulink package. Finally, the simulation results show that the proposed hybrid anti-islanding detection technique is capable of achieving higher detection efficiency as compared to any single detection techniques. The improvements include a narrower non-detected zone, faster response time and better power quality in terms of THDi.

ACKNOWLEDGMENT

The authors would like to express the greatest gratitude to the sponsorship of this research funding, the Research University Grant, granted by the Ministry of Education Malaysia under the vote of Q.J130000.2523.03H53 and Universiti Teknologi Malaysia (UTM).

REFERENCES

M.Asif, T.Muneer (2007), "Energy supply, its demand and security issues for developed and emerging economies". *Renewable and Sustainable Energy Reviews* 11, 1388-1413.

IEEE (2000), "IEEE Recommended Practice for Utility Interface of Photovoltaic (PV) Systems". *IEEE Std 929-2000*.

IEEE (2009), "IEEE Application Guide for IEEE Std 1547, IEEE Standard for Interconnecting Distributed Resources with Electric Power Systems". *IEEE Std 1547.2-2008*, 1-207.

AS (2005), "Australian Standard 4777.3-2005 Grid coonection of energy systems via inverters Part 3: Grid protection requirements". *AS 4777.3-2005*, 1-21.

IEEE (2003), "IEEE Standard for Interconnecting Distributed Resources With Electric Power Systems". *IEEE Std 1547-2003*, 0_1-16.

Skocil, T., Gomis-Bellmunt, O., Montesinos-Miracle, D., Galceran-Arellano, S., Rull-Duran, J. (2009), "Passive and active methods of islanding for PV systems". *Power Electronics and Applications, 2009. EPE '09. 13th European Conference on*, 1-10.

Ward Bower, Ropp., M. (2002a), "Evaluation of Islanding Detection Methods for Photovoltaic Utility Interactive Power systems". *IEA International Energy Agency,Task V Report IEA PVPS T509: 2002*.

A. S. Aljankawey, Walid G. Morsi, L. Chang, C.P. Diduch (2010), "Passive Method-based Islanding Detection of Renewable-based Distributed Generation: The Issues". *Electric Power and Energy Conference (EPEC), 2010 IEEE*, 1-8.

Mylène Robitaille, Kodjo Agbossou, Mamadou Lamine Doumbia, Simard, R. (2011), "Islanding Detection Method for a Hybrid Renewable Energy System". *International Journal of Renewable Energy Research, IJRER* Vol.1 , No.1, pp.41-53.

Velasco, D., Trujillo, C.L., Garcerá, G., Figueres, E. (2010), "Review of anti-islanding techniques in distributed generators". *Renewable and Sustainable Energy Reviews* 14, 1608-1614.

Luiz A.C.Lopes, Sun Huili (2006), "Performance Assessment of Active Frequency Drifting Islanding Detection Methods". *IEEE Transactions on Energy Conversion*, 21, 171-180.

Ward Bower, Ropp., M. (2002b), "Evaluation of Islanding Detection Methods for Utility-Interactive Inverters in Photovoltaic Systems". *SAND2002-3591 Unlimited Release*.

Kunte, R.S., Wenzhong, G. (2008), "Comparison and review of islanding detection techniques for distributed energy resources". *Power Symposium, 2008. NAPS '08. 40th North American*, 1-8.